

## Observation of TeV gamma-rays from the unidentified source HESS J1841-055 with the ARGO-YBJ experiment

B. Bartoli<sup>1,2</sup>, P. Bernardini<sup>3,4</sup>, X.J. Bi<sup>5</sup>, I. Bolognino<sup>6,7</sup>, P. Branchini<sup>8</sup>, A. Budano<sup>8</sup>, A.K. Calabrese Melcarne<sup>9</sup>, P. Camarri<sup>10,11</sup>, Z. Cao<sup>5</sup>, R. Cardarelli<sup>11</sup>, S. Catalanotti<sup>1,2</sup>, C. Cattaneo<sup>7</sup>, S.Z. Chen<sup>0,5</sup>, T.L. Chen<sup>12</sup>, Y. Chen<sup>5</sup>, P. Creti<sup>4</sup>, S.W. Cui<sup>13</sup>, B.Z. Dai<sup>14</sup>, G. D'Alì Staiti<sup>15,16</sup>, A. D'Amone<sup>3,4</sup>, Danzengluobu<sup>12</sup>, I. De Mitri<sup>3,4</sup>, B. D'Ettorre Piazzoli<sup>1,2</sup>, T. Di Girolamo<sup>1,2</sup>, X.H. Ding<sup>12</sup>, G. Di Sciascio<sup>11</sup>, C.F. Feng<sup>17</sup>, Zhaoyang Feng<sup>5</sup>, Zhenyong Feng<sup>18</sup>, F. Galeazzi<sup>8</sup>, E. Giroletti<sup>6,7</sup>, Q.B. Gou<sup>5</sup>, Y.Q. Guo<sup>5</sup>, H.H. He<sup>5</sup>, Haibing Hu<sup>12</sup>, Hongbo Hu<sup>5</sup>, Q. Huang<sup>18</sup>, M. Iacovacci<sup>1,2</sup>, R. Iuppa<sup>10,11</sup>, I. James<sup>8,19</sup>, H.Y. Jia<sup>18</sup>, Labaciren<sup>12</sup>, H.J. Li<sup>12</sup>, J.Y. Li<sup>17</sup>, X.X. Li<sup>5</sup>, G. Liguori<sup>6,7</sup>, C. Liu<sup>5</sup>, C.Q. Liu<sup>14</sup>, J. Liu<sup>14</sup>, M.Y. Liu<sup>12</sup>, H. Lu<sup>5</sup>, L.L. Ma<sup>5</sup>, X.H. Ma<sup>5</sup>, G. Mancarella<sup>3,4</sup>, S.M. Mari<sup>8,19</sup>, G. Marsella<sup>3,4</sup>, D. Martello<sup>3,4</sup>, S. Mastroianni<sup>2</sup>, P. Montini<sup>8,19</sup>, C.C. Ning<sup>12</sup>, A. Pagliaro<sup>16,20</sup>, M. Panareo<sup>3,4</sup>, B. Panico<sup>10,11</sup>, L. Perrone<sup>3,4</sup>, P. Pistilli<sup>8,19</sup>, F. Ruggieri<sup>8</sup>, P. Salvini<sup>7</sup>, R. Santonico<sup>10,11</sup>, S.N. Sbano<sup>3,4</sup>, P.R. Shen<sup>5</sup>, X.D. Sheng<sup>5</sup>, F. Shi<sup>5</sup>, A. Surdo<sup>4</sup>, Y.H. Tan<sup>5</sup>, P. Vallania<sup>21,22</sup>, S. Vernetto<sup>21,22</sup>, C. Vigorito<sup>22,23</sup>, B. Wang<sup>5</sup>, H. Wang<sup>5</sup>, C.Y. Wu<sup>5</sup>, H.R. Wu<sup>5</sup>, B. Xu<sup>18</sup>, L. Xue<sup>17</sup>, Q.Y. Yang<sup>14</sup>, X.C. Yang<sup>14</sup>, Z.G. Yao<sup>5</sup>, A.F. Yuan<sup>12</sup>, M. Zha<sup>5</sup>, H.M. Zhang<sup>5</sup>, Jilong Zhang<sup>5</sup>, Jianli Zhang<sup>5</sup>, L. Zhang<sup>14</sup>, P. Zhang<sup>14</sup>, X.Y. Zhang<sup>17</sup>, Y. Zhang<sup>5</sup>, J. Zhao<sup>5</sup>, Zhaxiciren<sup>12</sup>, Zhaxisangzhu<sup>12</sup>, X.X. Zhou<sup>18</sup>, F.R. Zhu<sup>18</sup>, Q.Q. Zhu<sup>5</sup> and G. Zizzi<sup>9</sup>  
(The ARGO-YBJ Collaboration)

---

<sup>0</sup>Corresponding author: S.Z. Chen, chensz@ihep.ac.cn

---

<sup>1</sup>Dipartimento di Fisica dell’Università di Napoli “Federico II”, Complesso Universitario di Monte Sant’Angelo, via Cinthia, 80126 Napoli, Italy.

<sup>2</sup>Istituto Nazionale di Fisica Nucleare, Sezione di Napoli, Complesso Universitario di Monte Sant’Angelo, via Cinthia, 80126 Napoli, Italy.

<sup>3</sup>Dipartimento Matematica e Fisica “Ennio De Giorgi”, Università del Salento, via per Arnesano, 73100 Lecce, Italy.

<sup>4</sup>Istituto Nazionale di Fisica Nucleare, Sezione di Lecce, via per Arnesano, 73100 Lecce, Italy.

<sup>5</sup>Key Laboratory of Particle Astrophysics, Institute of High Energy Physics, Chinese Academy of Sciences, P.O. Box 918, 100049 Beijing, P.R. China.

<sup>6</sup>Dipartimento di Fisica dell’Università di Pavia, via Bassi 6, 27100 Pavia, Italy.

<sup>7</sup>Istituto Nazionale di Fisica Nucleare, Sezione di Pavia, via Bassi 6, 27100 Pavia, Italy.

<sup>8</sup>Istituto Nazionale di Fisica Nucleare, Sezione di Roma Tre, via della Vasca Navale 84, 00146 Roma, Italy.

<sup>9</sup>Istituto Nazionale di Fisica Nucleare - CNAF, Viale Berti-Pichat 6/2, 40127 Bologna, Italy.

<sup>10</sup>Dipartimento di Fisica dell’Università di Roma “Tor Vergata”, via della Ricerca Scientifica 1, 00133 Roma, Italy.

<sup>11</sup>Istituto Nazionale di Fisica Nucleare, Sezione di Roma Tor Vergata, via della Ricerca Scientifica 1, 00133 Roma, Italy.

<sup>12</sup>Tibet University, 850000 Lhasa, Xizang, P.R. China.

<sup>13</sup>Hebei Normal University, Shijiazhuang 050016, Hebei, P.R. China.

<sup>14</sup>Yunnan University, 2 North Cuihu Rd., 650091 Kunming, Yunnan, P.R. China.

<sup>15</sup>Università degli Studi di Palermo, Dipartimento di Fisica, Viale delle Scienze, Edificio 18, 90128 Palermo, Italy.

<sup>16</sup>Istituto Nazionale di Fisica Nucleare, Sezione di Catania, Viale A. Doria 6, 95125 Catania, Italy.

<sup>17</sup>Shandong University, 250100 Jinan, Shandong, P.R. China.

<sup>18</sup>Southwest Jiaotong University, 610031 Chengdu, Sichuan, P.R. China.

<sup>19</sup>Dipartimento di Fisica dell’Università “Roma Tre”, via della Vasca Navale 84, 00146 Roma, Italy.

<sup>20</sup>Istituto di Astrofisica Spaziale e Fisica Cosmica dell’Istituto Nazionale di Astrofisica, via La Malfa 153, 90146 Palermo, Italy.

<sup>21</sup>Osservatorio Astrofisico di Torino dell’Istituto Nazionale di Astrofisica, corso Fiume 4, 10133 Torino, Italy.

<sup>22</sup>Istituto Nazionale di Fisica Nucleare, Sezione di Torino, via P. Giuria 1, 10125 Torino, Italy.

<sup>23</sup>Dipartimento di Fisica dell’Università di Torino, via P. Giuria 1, 10125 Torino, Italy.

## ABSTRACT

We report the observation of a very high energy  $\gamma$ -ray source, whose position is coincident with HESS J1841-055. This source has been observed for 4.5 years by the ARGO-YBJ experiment from November 2007 to July 2012. Its emission is detected with a statistical significance of 5.3 standard deviations. Parameterizing the source shape with a two-dimensional Gaussian function we estimate an extension  $\sigma = (0.40^{+0.32}_{-0.22})^\circ$ , consistent with the HESS measurement. The observed energy spectrum is  $dN/dE = (9.0 \pm 1.6) \times 10^{-13} (E/5 \text{ TeV})^{-2.32 \pm 0.23}$  photons  $\text{cm}^{-2} \text{ s}^{-1} \text{ TeV}^{-1}$ , in the energy range 0.9-50 TeV. The integral  $\gamma$ -ray flux above 1 TeV is  $1.3 \pm 0.4$  Crab units, which is  $3.2 \pm 1.0$  times the flux derived by HESS. The differences in the flux determination between HESS and ARGO-YBJ, and possible counterparts at other wavelengths are discussed.

*Subject headings:* gamma rays: general

## 1. Introduction

Very High Energy (VHE)  $\gamma$ -ray astronomy opened a new window to explore the extreme non-thermal phenomena in the universe. VHE  $\gamma$ -rays are tracers of non-thermal particle acceleration and are used to probe the conditions and the underlying astrophysical processes inside their sources. In the past decade, great progresses have been made in the field of VHE  $\gamma$ -ray astronomy. More than one hundred VHE  $\gamma$ -ray emitters have been detected, belonging to several categories: Active Galactic Nuclei (AGNs), Pulsar Wind Nebulae (PWNs), SuperNova Remnants (SNRs), X-ray Binaries (XBs), and starburst galaxies. However, there is a fraction of VHE sources still unidentified because do not appear to have obvious counterparts at other wavelengths. This kind of sources may constitute a new class of objects with different emission properties.

HESS J1841–055 is an enigmatic unidentified VHE  $\gamma$ -ray source discovered by the HESS collaboration during the Galactic plane survey (Aharonian et al. 2008). Its image shows a high extension, the measured axes for an elongated two-dimensional Gaussian shape being  $0.41^\circ \pm 0.04^\circ$  (major) and  $0.25^\circ \pm 0.02^\circ$  (minor). HESS J1841–055, therefore, is one of the most extended sources in the VHE  $\gamma$ -ray band. The spectrum is best fitted by a simple power law with photon index  $\alpha = -2.41 \pm 0.08$  in the energy range from 0.54 TeV to 80 TeV. The integral flux is  $9.1 \times 10^{-12}$  photons  $\text{cm}^{-2} \text{ s}^{-1}$  at energies above 1 TeV, about 40.3% of the Crab unit (Aharonian et al. 2006a).

To date, no obvious counterpart has been found at other wavelengths. The wide VHE  $\gamma$ -ray morphology suggests that HESS J1841–055 may be the blend of multiple sources. Aharonian et al. (2008) found four candidates which could be responsible for at least part of the entire VHE  $\gamma$ -ray emission: the two pulsars PSR J1841–0524 and PSR J1838–0549, the diffuse source G26.6–0.1, which is a candidate SNR basing on its ASCA spectrum, and finally the high-mass XB AX J1841.0–0536. Basing on a striking spatial correlation, Sguera et al. (2009) propose that the Supergiant Fast X-ray Transient (SFXT) AX J1841.0–0536 could be responsible for at least a fraction of the VHE  $\gamma$ -ray emission from HESS J1841–055, thus being the prototype of a new class of Galactic transient MeV/TeV emitters. Using  $\gamma$ -rays with energies  $> 100$  GeV detected by *Fermi*-LAT, Neronov & Semikoz (2010) found an event cluster adjacent to HESS J1841–055, and a more extended event cluster at the opposite side. This may be an evidence that HESS J1841–055 is composed of at least two different components. On the other hand, Neronov & Semikoz (2012) suggest an association only with PSR J1841–0524, which is situated in the center of the extended source.

The ARGO-YBJ experiment is an air shower array with large field of view (FOV) which continuously monitor the northern sky. The emission from the Crab Nebula has been detected with a statistical significance of 17 standard deviations (s.d.) at energies around 1 TeV. With such a sensitivity, other 4 known VHE  $\gamma$ -ray sources have been detected with significance greater than  $5\sigma$ : Mrk 421 (Bartoli et al. 2011a), Mrk 501 (Bartoli et al. 2012a), and the two extended sources MGRO J2031+41 (Bartoli et al. 2012b) and MGRO J1908+06 (Bartoli et al. 2012c). It should be pointed out that the fluxes of the two extended sources measured by the EAS arrays Milagro and ARGO-YBJ are much higher than that determined by the Cherenkov arrays, showing that there are some systematic differences between the two observation techniques for extended sources (Bartoli et al. 2012b,c; Abdo et al. 2012). Since also HESS J1841–055 is an extended source, its study would benefit from an observation using EAS arrays. HESS J1841–055 is observed by ARGO-YBJ, at the edge of its FOV, 4.8 hours per day with zenith angle less than  $50^\circ$ , culminating at  $35.7^\circ$ . This work presents the observation results for HESS J1841–055 with the ARGO-YBJ experiment.

## 2. The ARGO-YBJ experiment

The ARGO-YBJ experiment is a full coverage extensive air shower array resulting from a collaboration between Chinese and Italian institutions and is designed for VHE  $\gamma$ -ray astronomy and cosmic ray observations. The detector is operating at the Yangbajing International Cosmic Ray Observatory (Tibet, P.R. China), at an altitude of 4300 m a.s.l.. The detector, extensively described in (Aielli et al. 2006, 2009c), consists of a single layer of Resistive

Plate Chambers (RPCs,  $2.8 \text{ m} \times 1.25 \text{ m}$ ), equipped with 10 logical pixels (called “pads”,  $55.6 \text{ cm} \times 61.8 \text{ cm}$ ) used for triggering and timing purposes. 130 clusters (each composed by 12 RPCs) are installed to form the central carpet of  $74 \text{ m} \times 78 \text{ m}$  with an active area of  $\sim 93\%$ , surrounded by 23 additional clusters (“guard ring”). The total area of the array is  $110 \text{ m} \times 100 \text{ m}$ . The arrival time of the particles is measured by time-to-digital converters (TDCs) with a resolution of about 1.8 ns (Aielli et al. 2009c). To calibrate the 18,360 TDC channels, a software method has been developed using cosmic ray showers (He et al. 2007). The calibration precision is 0.4 ns and the procedure is applied every month (Aielli et al. 2009a).

The central 130 clusters started taking data in July 2006, while the complete ARGO-YBJ detector including the “guard ring” collected data since November 2007. The RPC carpet is connected to two independent data acquisition systems, corresponding to the shower and scaler operation modes (Aielli et al. 2008). In the current work, only data from the shower mode are used. In shower mode, the ARGO-YBJ detector is operated by requiring at least 20 fired pads ( $N_{pad}$ ) within 420 ns on the entire carpet detector. The trigger rate is 3.5 kHz with a dead time of 4% and the average duty-cycle is higher than 86%.

The high granularity of the apparatus allows a complete and detailed space-time three-dimensional reconstruction of the shower profile and therefore of the incident direction of the primary particle. Through the analysis of the position, size and shape of the reconstructed Moon and Sun shadows in the cosmic ray flux, the angular resolution, pointing accuracy and stability of the ARGO-YBJ detector array have been thoroughly tested (Bartoli et al. 2011b; Aielli et al. 2011). The Point Spread Function (PSF) is quantified using a parameter  $\psi_{70}$  as the opening angle containing 71.5% of the events. For cosmic ray-induced air showers  $\psi_{70}$  is  $2.8^\circ$  for  $N_{pad} \sim 20$ , while becomes  $0.47^\circ$  for  $N_{pad} > 1000$  (Bartoli et al. 2011a,b), in good agreement with Monte Carlo predictions. The simulations show that the angular resolution for  $\gamma$ -induced showers is 30–40% smaller. The effective area of the detector for  $\gamma$ -induced showers depends on the  $\gamma$ -ray energy and incident zenith angle, e.g., it is about  $100 \text{ m}^2$  at 100 GeV and  $>10,000 \text{ m}^2$  above 1 TeV for a zenith angle of  $20^\circ$  (Aielli et al. 2009b).

### 3. Data analysis

The data set used in this analysis refers to the period from November 2007 to July 2012. The total effective observation time is 1492.6 days. For the analysis presented in this paper, only events with a zenith angle less than  $50^\circ$  are used, and the data set is divided into six groups according to  $N_{pad}$ . To achieve a good angular resolution, the event selections used in (Bartoli et al. 2011a) are applied here. The total number of events after filtering used in this

work is  $2.42 \times 10^{11}$ . The opening angles  $\psi_{70}$  for events with  $N_{pad} > 60$  and  $N_{pad} > 100$  are  $1.36^\circ$  and  $0.98^\circ$ , respectively. For the data set in each group, the whole sky map in celestial coordinates (right ascension and declination) is divided into a grid of  $0.1^\circ \times 0.1^\circ$  bins and filled with detected events according to their reconstructed arrival direction. The “direct integral method” (Fleysher et al. 2004) is adopted to estimate the cosmic-ray background and to extract the excess of  $\gamma$ -induced showers from each bin. The correction procedure described in (Bartoli et al. 2011a) has been applied to remove the effect of cosmic ray anisotropy on a scale of  $11^\circ \times 11^\circ$ . A Gaussian smoothing method is used to take into account the PSF of the ARGO-YBJ detector. That is, the events in a circular area centered on the bin with an angular radius of  $1.3\psi_{70}$ , are summed after weighting with the Gaussian-shaped PSF. The Li-Ma method (Li & Ma 1983) is used to estimate the significance of the excess in each bin.

With this procedure, the northern sky has been surveyed (Cao & Chen 2011). The significance of the excess observed from the direction of the Crab Nebula is 17 s.d., indicating that the cumulative 5 s.d. sensitivity of ARGO-YBJ has reached 0.3 Crab unit for point sources. The sensitivity is dependent on the declination of the source, being degraded by a factor 3.5 at the declination of HESS J1841–055 (Cao & Chen 2011). For an extended source with a symmetrical two-dimensional Gaussian shape with  $\sigma = 0.40^\circ$ , the sensitivity is degraded by 15%. Therefore, a simple estimation indicates that the flux from HESS J1841–055 should be about 1.2 Crab units in order to be detected by ARGO-YBJ with 5 s.d.. The required flux slightly varies if the spectrum is different from that of the Crab Nebula.

#### 4. Results

The significance map around HESS J1841–055, as observed by ARGO-YBJ using events with  $N_{pad} > 60$ , is shown in Figure 1. For comparison, the twelve sources in the second *Fermi*-LAT catalog (Nolan et al. 2012) around HESS J1841–055 are also marked in the figure. Weak excesses are observed along the Galactic plane, indicating a diffuse  $\gamma$ -ray emission. An analysis of the diffuse  $\gamma$ -ray emission using ARGO-YBJ data can be found in (Ma 2011). The highest significance is 5.3 s.d. at  $\alpha=18^h39^m$  and  $\delta=-6^\circ3'$  (J2000), which is displaced  $0.7^\circ$  from the center of HESS J1841–055. To estimate the statistical error of the position, the data are sampled 20,000 times and the statistical errors in both directions are about  $0.45^\circ$ . However, most of the excesses overlap the extended region of HESS J1841–055 and its gravity center ( $\alpha=18^h40^m \pm 12^m$  and  $\delta=-5^\circ52' \pm 13'$ ), obtained using all the pixels with significance greater than 3 s.d. within  $3^\circ \times 3^\circ$  around HESSJ1841–055, is  $0.4^\circ$  off the center of HESS J1841–055. These displacements may be caused by different concurring effects beside

fluctuation. (1) Complex morphology. According to the HESS result, HESS J1841–055 possibly has two or three peaks and the positions of the two largest ones are both  $0.44^\circ$  off the center. (2) The systematic pointing error of ARGO-YBJ is  $0.2^\circ$ , slightly increasing at the boundary of the ARGO-YBJ FOV. (3) The contribution of the nearby VHE source HESS J1837–069, partially containing its emission. Therefore, the signal position observed by ARGO-YBJ largely overlaps HESS J1841–055.

The intrinsic extension of HESS J1841–055 is determined by fitting the distribution of  $\theta^2$  for the events exceeding the background as shown in Figure 2, where  $\theta$  is the angular distance of each event to the position of HESS J1841–055. To achieve a good angular resolution, only events with  $N_{pad} > 100$  are used in this fit. In order to fit the data, a set of  $\gamma$ -rays is generated taking into account the Spectral Energy Distribution (SED), the intrinsic source extension, and the detector PSF. The extension is estimated by minimizing the  $\chi^2$  between data and generated events, from  $0^\circ$  to  $1^\circ$  with steps of  $0.1^\circ$ . Assuming a spectral index  $-2.3$ , the intrinsic extension is determined to be  $\sigma_{ext} = (0.40^{+0.32}_{-0.22})^\circ$ . It is found that the dependence on the SED is negligible within the uncertainties. This result is consistent with the estimation by the HESS collaboration, i.e.,  $0.41^\circ \pm 0.04^\circ$  and  $0.25^\circ \pm 0.02^\circ$  along the major and minor axes, respectively (Aharonian et al. 2008).

Assuming an intrinsic extension  $\sigma_{ext} = 0.40^\circ$ , we estimate the spectrum of HESS J1841–055 using the ARGO-YBJ data with the conventional fitting method described in (Bartoli et al. 2011a). In this procedure, the expectation function is generated by sampling events in the energy range from 10 GeV to 100 TeV and taking into account the detailed ARGO-YBJ detector response, assuming a power law with its spectral index as a parameter. We define five  $N_{pad}$  intervals: 60–59, 100–199, 200–499, 500–999, and  $\geq 1000$ . The best fit to the SED and the corresponding  $1\sigma$  error region are shown in Figure 3. The differential flux ( $\text{TeV}^{-1} \text{ cm}^{-2} \text{ s}^{-1}$ ) in the energy range from 0.9 TeV to 50 TeV is

$$\frac{dN}{dE} = (9.0 \pm 1.6) \times 10^{-13} (E/5 \text{ TeV})^{-2.32 \pm 0.23}. \quad (1)$$

The median energies of the five  $N_{pad}$  intervals are 2.3, 3.5, 7.1, 14 and 22 TeV, respectively. The integral flux is  $1.3 \pm 0.4$  Crab units at energies above 1 TeV, which is  $3.2 \pm 1.0$  times the flux determined by the HESS experiment, i.e., 0.40 Crab unit.

## 5. Discussion

The integrated energy flux above 1 TeV measured by ARGO-YBJ is  $\sim 1.9 \times 10^{-10} \text{ erg cm}^{-2} \text{ s}^{-1}$ , corresponding to a source luminosity, assuming isotropic emission, of  $L(>1 \text{ TeV}) \sim 2.3 \times 10^{34} (D/1 \text{ kpc})^2 \text{ erg s}^{-1}$ , where  $D$  is the distance to the source. However, due to

the limitations in the angular resolution, this flux may also include other contributions apart from HESS J1841–055. Diffuse  $\gamma$ -rays, produced by cosmic rays interacting with matter in the Galaxy plane, are expected to contribute to the ARGO-YBJ result. According to the measurement of diffuse  $\gamma$ -ray flux from the inner Galactic plane using ARGO-YBJ data (Ma 2011), this contribution to the flux from HESS J1841–055 in the five intervals is less than 4%. Assuming the HESS shape for the source instead of the symmetrical two-dimensional Gaussian shape, the flux would only vary of 2.2%. HESS J1837–069 is the nearest VHE  $\gamma$ -ray source with an angular distance of 1.62 degrees. The flux from HESS J1837–069 at energies above 1 TeV is 17% that of the Crab with spectral index  $-2.27$  (Aharonian et al. 2006b). Its contributions to the five intervals are estimated to be 5.8%, 2.7%, 1.0%, 0.7%, and 0.2%, respectively. The second nearest source is HESS J1843-033, whose flux is still unknown. A hot spot with a marginal significance of 4.1 s.d. is observed near its position (Hoppe et al. 2007). With an angular separation of 2.6 degrees, its contribution is estimated to be lower compared with HESS J1837–069. The contribution from other known VHE  $\gamma$ -ray sources is negligible. Moreover, an estimate of the systematic error of ARGO-YBJ is described in (Bartoli et al. 2012b). With an incomplete list of possible causes, such as time resolution variation, event rate variation with environment parameters, and pointing error, the systematic error for point sources is found to be less than 30%, and is lower for extended sources. Thus, the systematic error of ARGO-YBJ alone is not enough to explain the discrepancy.

HESS J1841-055 is observed by ARGO-YBJ only at high zenith angles ( $\theta > 35.7^\circ$ ), while the observation of the Crab is possible also at low zenith angles. This difference may cause some systematic errors when estimating the spectrum of HESS J1841-055. To check a possible systematic error, observations of the Crab at zenith angles higher than  $30^\circ$  are used. With this selection, the average zenith angle is about the same as that of HESS J1841-055. The result is that the Crab spectral index varies from  $(2.58 \pm 0.07)$  to  $(2.52 \pm 0.21)$ , and the flux above 1 TeV is  $(35 \pm 28)\%$  higher. Due to the large statistical error, we cannot exclude a systematic effect causing the difference of flux. However, even taking this systematic error into account, the flux of HESS J1841-055 observed by ARGO-YBJ is still about twice that determined by HESS.

On the other hand, the discrepancy is similar to that found for the two extended sources MGRO J1908+06 and MGRO J2031+41 (Bartoli et al. 2012c,b). The fluxes measured by the EAS arrays Milagro and ARGO-YBJ are much higher than that determined by the Cherenkov arrays. Since a good agreement has been achieved on the “standard candle” Crab Nebula, some systematic differences between the two techniques should exist only for extended sources. As pointed out by Abdo et al. (2012), due to their limited FOV, Cherenkov telescopes might count the extended emission as background, especially when using the



“wobble mode” to estimate this latter. It is worth noting that the “wobble mode” was used when HESS observed HESS J1841–055, and the source was offset by  $0.7^\circ$  (Aharonian et al. 2008). The “reflected-region technique” is used to estimate the background for spectra in a region partially overlapping the extended source. As a result, HESS would measure an emission fainter than that measured by ARGO-YBJ.

Different scenarios have been proposed to explain the emission mechanism of TeV photons. VHE  $\gamma$ -rays can be produced via inverse-Compton of background photon fields by high energy electrons, or, in hadronic models, by inelastic proton-proton or proton-photon interactions. In both scenarios, X-ray and radio synchrotron emissions are expected, therefore the lack of a low energy counterpart for HESS J1841–055 poses the question about the nature of the emission mechanism. Aharonian et al. (2008) searched for counterparts responsible of the VHE  $\gamma$ -ray emission and discussed the possible association with six candidates, marked in Figure 4, which is a zoom of Figure 1 around HESS J1841–055. Three of them are the pulsars PSR J1838–0549, PSR J1841–0524 and PSR J1837–0604, of which only the last has a high enough spin-down flux ( $\dot{E}/D^2 = 5.2 \times 10^{34} \text{ erg s}^{-1} \text{ kpc}^{-2}$ ) to be a counterpart candidate. This source is at the boundary of the HESS region, but not far from the center of gravity of the ARGO-YBJ signal. However, as pointed out in (Aharonian et al. 2008), since the TeV emission is usually attributed to a relic population of electrons, some contribution can be expected also from the other pulsars if they had a much higher spin-down luminosity in the past. No catalogued PWNs at longer wavelengths are associated to these pulsars, however, according to the recent calculations of (Tibolla et al. 2012), during their evolution ancient PWNs ( $>>10 \text{ kyr}$ ) might appear as GeV-TeV  $\gamma$ -ray sources without X-ray counterpart. The three other catalogued objects located inside the HESS uncertainty region are the SNR G027.4 (also known as Kes73), the high-mass XB AX J1841.0–0536 and the diffuse source G26.6-0.1. The SNR Kes73 lies at the edge of the TeV emission region. The point-like nature of AX J1841.0–0536, the only soft  $\gamma$ -ray source detected within the HESS J1841–055 error ellipse, its variability and the required luminosity (about  $10^{36} \text{ erg s}^{-1}$  according to the ARGO-YBJ data and assuming a distance of 6.9 kpc as inferred in (Sguera et al. 2009)) exclude its association with the entire emission from the extended HESS source. Also the diffuse source G26.6-01, at only 1.3 kpc and well inside the emission region, could be responsible at least for part of the TeV flux. In Figure 4 are also reported four GeV  $\gamma$ -ray sources from the *Fermi*-LAT second source catalogue within the extension of HESS J1841–055: 2FGL J1839.3–0558c, 2FGL J1836.8–0623c, and the two diffuse sources 2FGL J1839.0–0539 and 2FGL J1841.2–0459c (Nolan et al. 2012). Moreover, the two event clusters at energies above 100 GeV found by (Neronov & Semikoz 2010) are shown. Three GeV sources are within the two event clusters, suggesting that they may be also VHE emitters: 2FGL J1841.2–0459c is coincident with the SNR Kes 73, while 2FGL J1839.3–0558c

and 2FGL J1839.0–0539 are spatially associated to the PSR J1838-0549 and the diffuse X-ray G26.6–0.1, respectively. As remarked in (Tibolla et al. 2012), the recent observation by *Fermi*-LAT of GeV sources not firmly associated to X-ray counterparts suggests that VHE unidentified sources can be explained as ancient PWNs.

An hadronic scenario is proposed in (Neronov & Semikoz 2012). These authors consider the extended  $\gamma$ -ray emission produced by high-energy cosmic rays escaping from the source and diffusing in the interstellar medium (ISM). The  $\gamma$ -ray emission should result from the interaction of these cosmic rays with the ISM particles. Such extended emission regions should be visible as VHE  $\gamma$ -ray sources with fluxes of order  $10^{-11}$  erg cm $^{-2}$  s $^{-1}$  above 100 GeV. From the analysis of the *Fermi*-LAT data they suggest the young nearby pulsar PSR J1841–0524 as a possible low energy counterpart of HESS J1841–055. However, as already stated, due to the energy balance, this association is not without problems. The proton/nuclei contribution to the extended  $\gamma$ -ray flux should generate a comparable flux of TeV neutrinos with a spectrum expected to follow the  $\gamma$ -ray spectrum. Thus, the observation of high energy neutrinos from the HESS source could provide a crucial test to this model. A search for individual neutrino sources over a large fraction of both the northern and southern skies has been carried out by the IceCube detector in the 40-string configuration (Abbasi et al. 2011). The large background from atmospheric muons reduces the IceCube sensitivity to neutrino sources in the southern sky at TeV energies, thus the derived upper limits are not stringent enough to constrain the hadronic scenario. Data from the combined operation of IceCube and AMANDA have been used to scan for sources in the Galactic plane (Abbasi et al. 2012) with a neutrino flux sensitivity of about  $10^{-11} - 10^{-12}$  erg cm $^{-2}$  s $^{-1}$  at TeV energies. However, the surveyed range of Galactic longitude ( $36^\circ < l < 210^\circ$ ) does not include the region where HESS J1841–055 is located.

In the case of hadronic scenarios one expects the source extension to be much larger than seen by Cherenkov telescopes (up to the degree scale). Therefore, the lower angular resolution and the large FOV of ARGO-YBJ allows the collection of photons from a larger source area. This could partially explain the discrepancy in flux with the HESS Cherenkov telescope.

Recently, Giacinti et al. (2012) found that diffusion of cosmic rays and electrons around point sources is strongly anisotropic and shows filamentary structures, which may cause the shift of the centroid position between HESS and ARGO-YBJ.

## 6. Conclusions

Since November 2007 the ARGO-YBJ experiment is monitoring with high duty cycle the northern sky at TeV photon energies. Using data up to July 2012, an excess with statistical significance of 5.3 s.d. is detected from the direction of the unidentified source HESS J1841–055. The source location and extension are consistent with those determined by HESS, however the measured flux above 1 TeV is about 3 times higher. This discrepancy, already found in the observation of other extended sources, could origin from the different techniques used in the background estimation for extended sources with ARGO-YBJ and HESS data. The extended morphology of HESS J1841–055 and the presence of several sources within the 90% confidence error region suggests contributions from more than one of them, but so far no clear counterparts in lower-energy wavebands can be identified. However, the possibility of a GeV-TeV  $\gamma$ -ray source without any counterpart can not be excluded. Both leptonic and hadronic productions of  $\gamma$ -rays have been proposed, but it is not easy to distinguish between the two contributions basing only on the  $\gamma$ -ray data. The current upper limits to the neutrino flux from the HESS J1841–055 region are too high to test the hadronic model. Further multiwavelength observations from radio to GeV energies and data from neutrino telescopes of suitable sensitivity are needed in order to disentangle between the different emission possibilities.

This work is supported in China by NSFC (No.10120130794, No.11205165), the Chinese Ministry of Science and Technology, the Chinese Academy of Sciences, the Key Laboratory of Particle Astrophysics, CAS, and in Italy by the Istituto Nazionale di Fisica Nucleare (INFN).

We also acknowledge the essential supports of W.Y. Chen, G. Yang, X.F. Yuan, C.Y. Zhao, R. Assiro, B. Biondo, S. Bricola, F. Budano, A. Corvaglia, B. D’Aquino, R. Esposito, A. Innocente, A. Mangano, E. Pastori, C. Pinto, E. Reali, F. Taurino and A. Zerbini, in the installation, debugging and maintenance of the detector.

## REFERENCES

- Abbasi, R., et al. 2011, ApJ, 732, 18
- Abbasi, R., et al. 2012, arXiv:1210.3273
- Abdo, A. A., et al. 2012, ApJ, 753, 159
- Aharonian, F., et al. 2006a A&A, 457, 899

- Aharonian, F., et al. 2006b *ApJ*, 636, 777
- Aharonian, F., et al. 2008, *A&A*, 477, 353
- Aielli, G., et al. 2006, *Nucl. Instrum. Meth. A*, 562, 92
- Aielli, G., et al. 2008, *Astrop. Phys.*, 30, 85
- Aielli, G., et al. 2009a, *Astrop. Phys.*, 30, 287
- Aielli, G., et al. 2009b, *Astrop. Phys.*, 32, 47
- Aielli, G., et al. 2009c, *Nucl. Instrum. Meth. A*, 608, 246
- Aielli, G., et al. 2011, *ApJ*, 729, 113
- Bartoli, B., et al. 2011a, *ApJ*, 734, 110
- Bartoli, B., et al. 2011b, *Phys. Rev. D*, 84, 022003
- Bartoli, B., et al. 2012a, *ApJ*, 758, 2
- Bartoli, B., et al. 2012b, *ApJ*, 745, L22
- Bartoli, B., et al. 2012c, *ApJ*, 760, 110
- Cao, Z., & Chen, S.Z. 2011, in *Proc. 32nd ICRC*, (available at <http://icrc2011.ihep.ac.cn>, arXiv:1110.1809v1)
- Fleysher, R., Fleysher, L., Nemethy, P., & Mincer, A.I., 2004, *ApJ*, 603, 355
- Giacinti, G., Kachelrieß, M., & Semikoz, D.V. 2012, *Phys. Rev. Lett.*, 108, 261101
- He, H. H., Bernardini, P., Calabrese Melcarne, A. K., & Chen, S. Z. 2007, *Astropart. Phys.*, 27, 528
- Hoppe, S., 2007, in *Proc. 30th ICRC*, ed. R. Caballero et al. (Mexico City: Univ. Nacional Autonoma de Mexico), 579
- Li, T.P., & Ma, Y.Q. 1983, *ApJ*, 272, 317
- Ma, L.L. 2011, in *Proc. 32nd ICRC*, (available at <http://icrc2011.ihep.ac.cn>)
- Neronov, A., & Semikoz, D., 2010, arXiv:1011.0210
- Neronov, A., & Semikoz, D., 2012, *Phys. Rev. D*, 85, 083008

Nolan, P. L., et al. 2012, ApJS, 199, 31

Sguera, V., Romero, G.E., Bazzano, A., Masetti, N., Bird, A.J., & Bassani, L., 2009, ApJ, 697, 1194

Tibolla, O., et al. 2012, in Proc. 5th International Symposium on High-Energy Gamma-Ray Astronomy (arXiv:1210.1378)

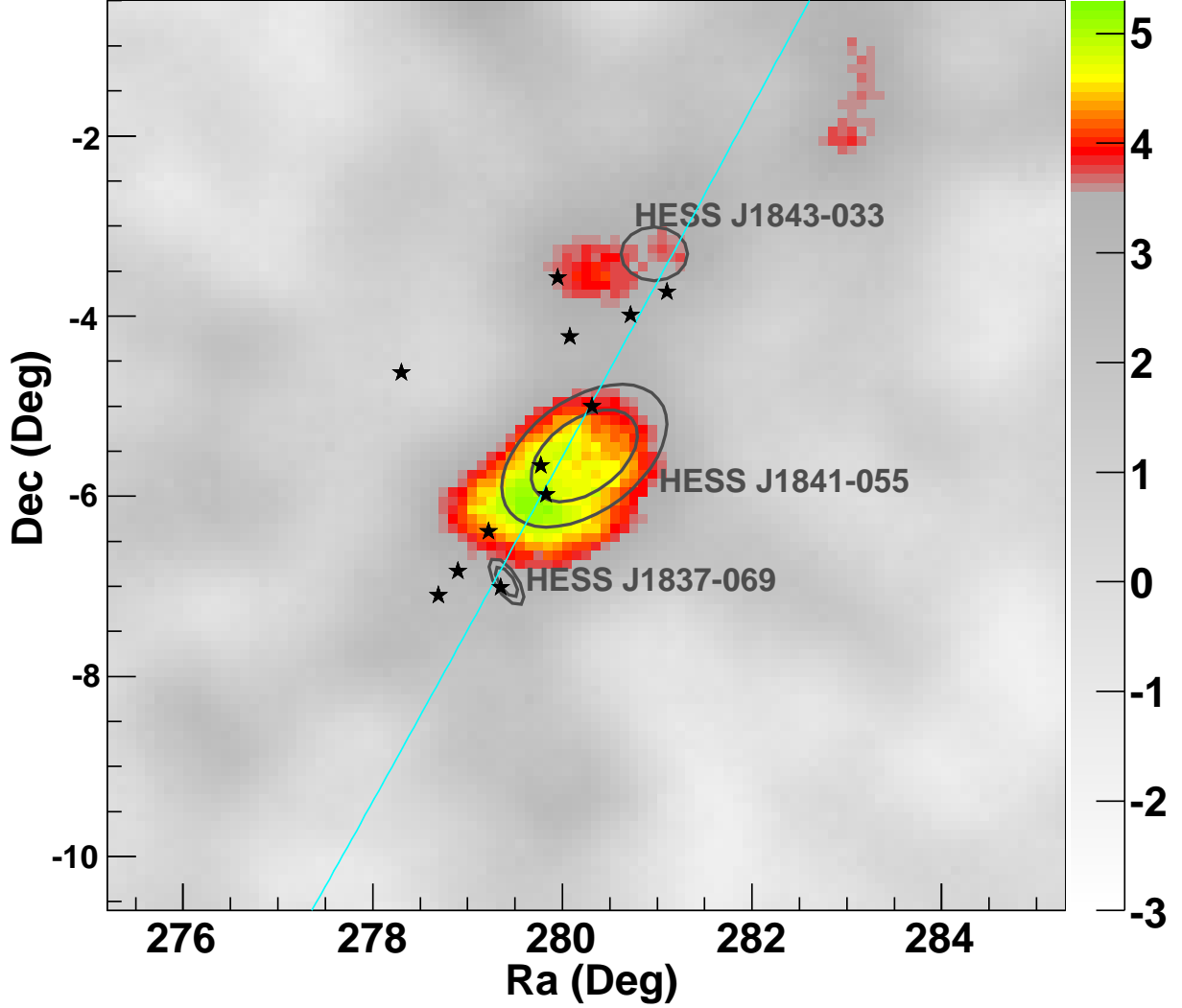


Fig. 1.— The significance map around HESS J1841–055 as observed by the ARGO-YBJ experiment. The two ellipses for HESS J1841–055 and HESS J1837–069 indicate their positions and the 68% and 90% contours of their extension regions (Aharonian et al. 2008). The position and possible extension of HESS J1843–33 are marked with ellipse (Hoppe et al. 2007). The stars mark the location of the GeV  $\gamma$ -ray sources around HESS J1841–055 in the second *Fermi*-LAT catalog (Nolan et al. 2012). The solid line indicates the Galactic plane.

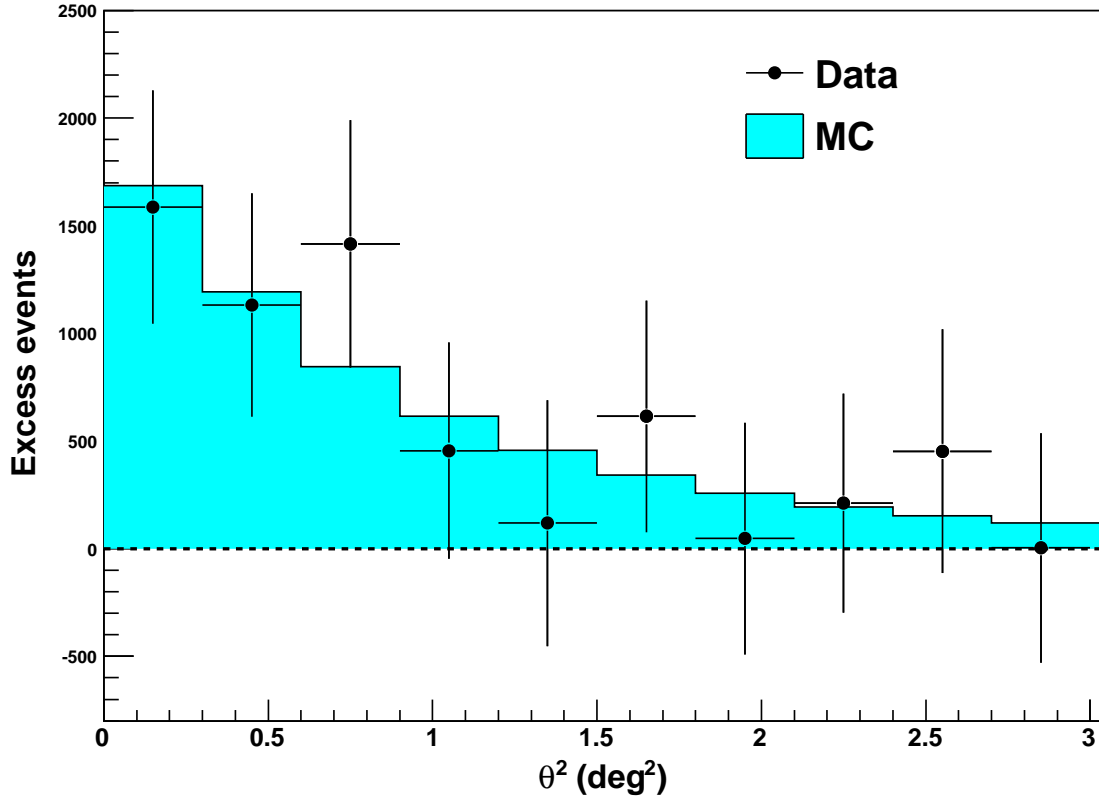


Fig. 2.— Distribution of  $\theta^2$  for the number of excess events around HESS J1841–055. The filled region outline the best fit to simulated data assuming a symmetrical two-dimensional Gaussian shape with  $\sigma = 0.40^\circ$ .

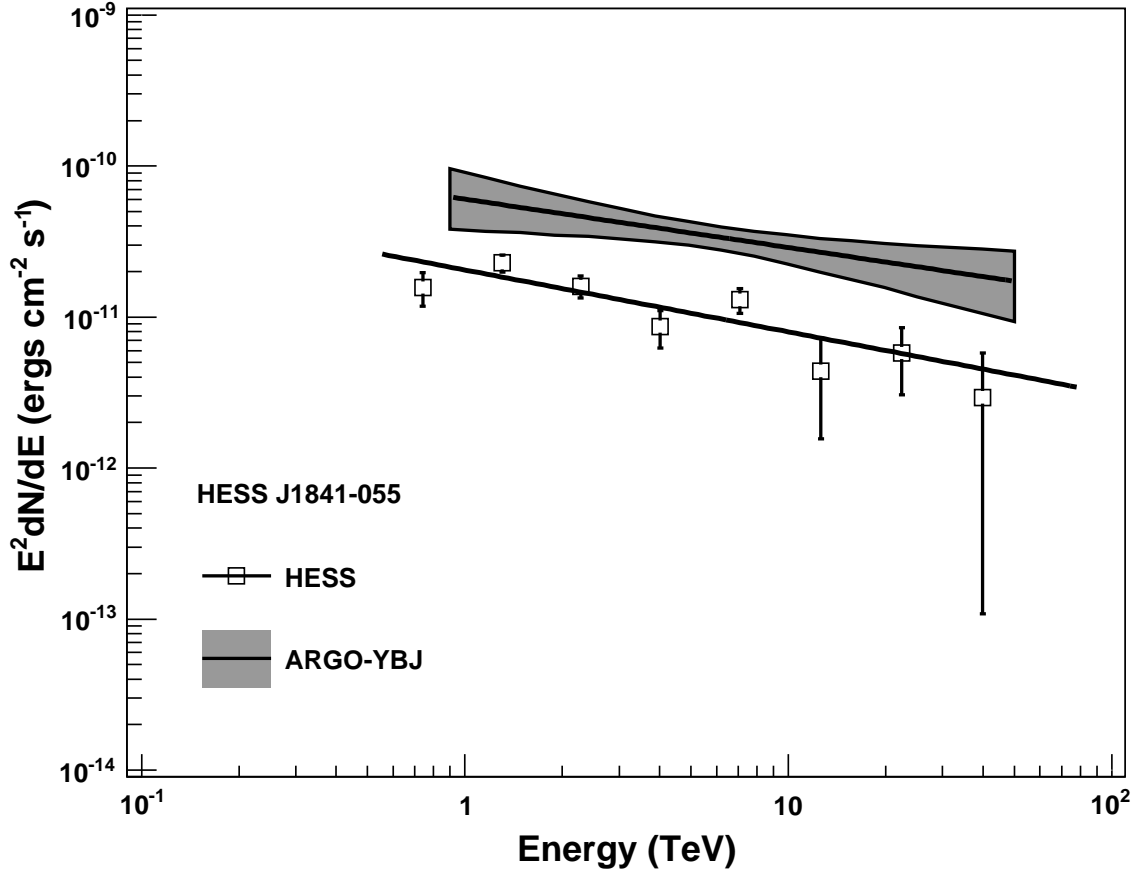


Fig. 3.— Energy density spectrum of HESS J1841–055 as measured by the ARGO-YBJ experiment: the solid line and shaded area indicate the differential energy spectrum and the 1 s.d. error region. The spectrum measured by HESS (Aharonian et al. 2008) is also reported for comparison. Only statistical errors are shown.



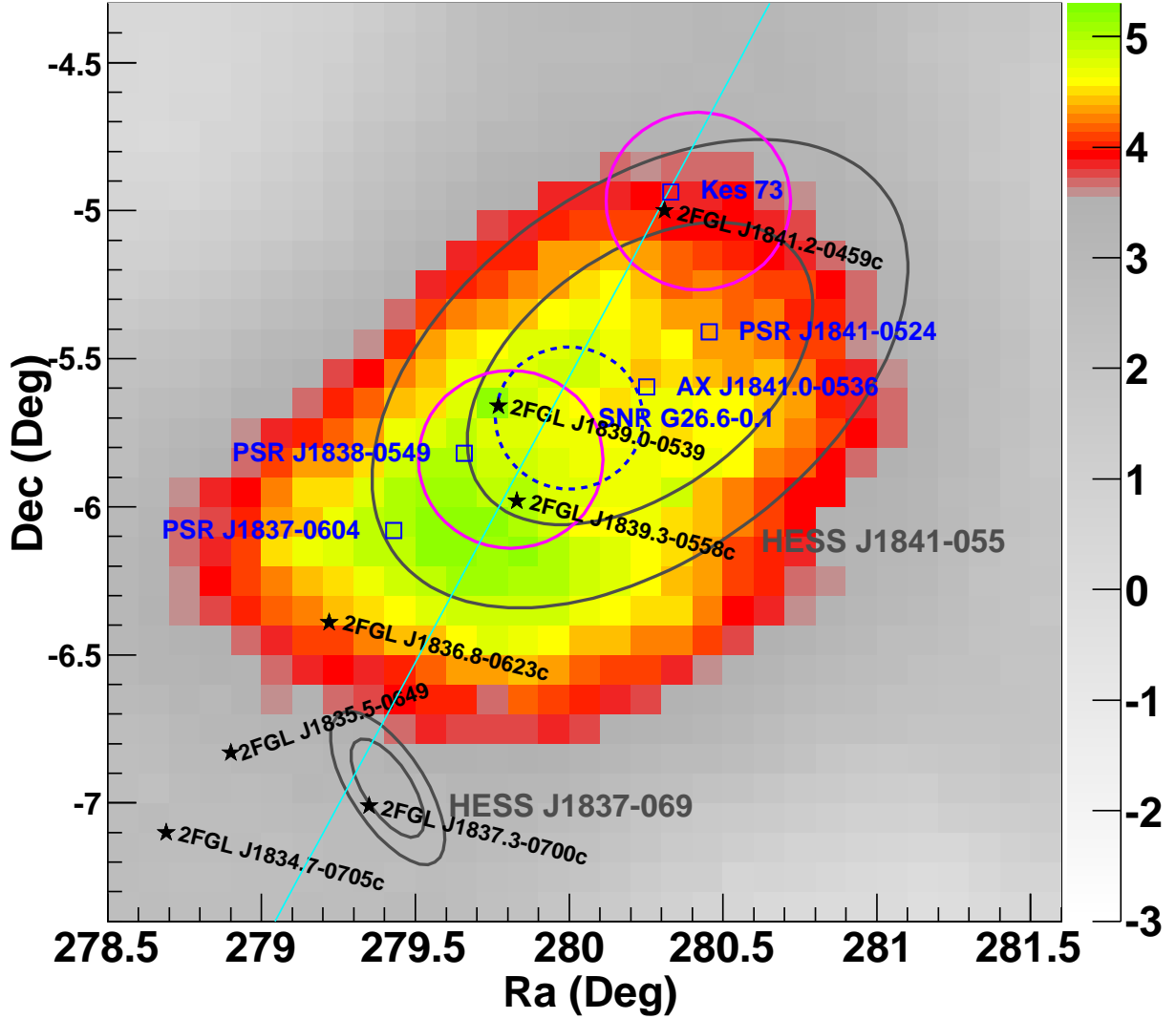


Fig. 4.— Zoom of Figure 1 around HESS J1841–055. The squares and the dashed circle indicate the position of the candidates reported in (Aharonian et al. 2008). The circles indicate the two event clusters found in (Neronov & Semikoz 2010) at energies above 100 GeV. The ellipses and stars are the same as in Figure 1. The solid line indicates the Galactic plane.